J Solid State Electrochem (1998) 2: 156–161

ORIGINAL PAPER

Sung-Mo Moon · Su-Il Pyun

Growth mechanism of anodic oxide films on pure aluminium in aqueous acidic and alkaline solutions

Received: 12 August 1997 / Accepted: 9 October 1997

Abstract The present work was conducted to explore the growth mechanism of anodic oxide films on pure aluminium in aqueous acidic and alkaline solutions by using a.c. impedance spectroscopy and a beam deflection technique. From the analyses of a.c impedance data, it was found that the reciprocal capacitance of anodic oxide film on pure aluminium increased linearly with increasing film formation potential in both acidic and alkaline solutions, indicating a linear increase in the film thickness with film formation potential. However, as the film formation potential increased, the resistance of anodic oxide film decreased in acidic solution, while it increased in alkaline solution. From the measurements of the deflection, the deflection was observed to move towards only a compressive direction with time in acidic solution, but it showed a transition in the direction of movement from compressive to tensile in alkaline solution. Based upon the above experimental results, it is suggested that the movement of oxygen vacancy through the oxide film contributes to the growth of anodic oxide film on pure aluminium in acidic solution, but the movement of both aluminium vacancy and oxygen vacancy accounts for that oxide film growth in alkaline solution.

Key words Aluminium · Aqueous solution · A.c. impedance spectroscopy · Beam deflection technique · Anodic oxide film

Introduction

When an anodic current density is applied to valve metals, such as aluminium, tantalum, titanium and zirconium, in aqueous solutions, anodic oxide films are developed on their surfaces which lead to improved resistance to corrosion. The oxide films anodically formed on valve metals have been of great interest in relation to their industrial applications, and thus the growth mechanism of anodic oxide films has been extensively investigated by many authors [1–8].

The growth kinetics of anodic oxide films was first described by the work of Cabrera and Mott [1], in which the transport of ions through the oxide film is driven by high electric field. The high-field ion conduction model has been modified by Kirchheim [7] and developed by others [4, 5]. On the other hand, the point defect model [6] was suggested to account for the film growth kinetics, in which the migrations of metal vacancy and oxygen vacancy through the oxide film result in dissolution of the metal and formation of the oxide film, respectively. By contrast, Pyun and Hong [8] showed that the migration of cation vacancy could contribute not only to the metal dissolution but also to the oxide film formation.

It is known that aluminium vacancy and oxygen vacancy are simultaneously present within anodic oxide films on aluminium [9–11]. It was reported that aluminium vacancies are generated at the oxide filk/solution interface in acidic solutions as a consequence of a field-assisted oxide dissolution which involves direct ejection of aluminium ions from the oxide film into the solution [12–14]. However, since aluminium ions are not thermodynamically stable in alkaline solution [15], the generation of aluminium vacancy due to direct ejection of aluminium ions into the solution will hardly occur in alkaline solution. So, aluminium vacancy within the oxide film in alkaline solution is expected to be generated by another electrochemical reaction at the oxide film/solution interface. Thus, the growth mechanism of the anodic oxide film in acidic solution may be different from that in alkaline solution.

The present work is aimed at elucidating the growth mechanism of anodic oxide films on pure aluminium in acidic and alkaline solutions. For this purpose, the

S.-M. Moon · S.-I. Pyun (✉)
Department of Materials Science and Engineering,
Korea Advanced Institute of Science and Technology,
373-1 Kusong-Dong, Yusong-Gu, Daejon 305-701, Korea

resistance and capacitance of anodic oxide film were determined from the analyses of a.c. impedance data, and the deflection and the corresponding potential of the specimen were simultaneously measured with time at various applied anodic current densities in acidic and alkaline solutions.

Experimental

Two kinds of specimens were made from 99.999% purity aluminium rod (Aldrich) of 6.35 mm diameter and from 99.99% purity aluminium foil (Aldrich) of 0.13 mm thickness for a.c. impedance measurements and for the deflection measurements, respectively. The rod specimen was annealed at 350 °C for 2 h in a vacuum furnace and then was set in a block of polyethylene. The upper surface of the block was ground with successively finer silicon carbide paper, ending with 2000 grit, to expose the cross section of the electrode to the electrolytic solution.

The pure aluminium foil was cut into strips with dimensions of 2.5 mm × 100 mm. Each strip specimen was lightly rolled between a clean ground glass stopper and a sheet of glass to smooth the burrs produced by cutting, and then annealed at 350 °C for 2 h in a vacuum furnace to remove residual stresses, followed by furnace cooling. The annealed strip specimen was etched for 2 mm in 10^{-1} M NaOH solution. After these treatments, the strip specimen was coated on one side with a fast-drying lacquer to make that side inert. After the lacquer had dried, a small mirror of silvered mica was attached to the coated side about 1.3 cm away from the end of the strip specimen. The mirror was used for the measurements of the deflection of the strip specimen during anodic oxidation of pure aluminium.

In all the electrochemical experiments, the annealed rod and strip specimens were used as the working electrode. A platinum gauze and a saturated calomel electrode (SCE) served as the counter and reference electrodes, respectively. The electrolytes used in this study were 5×10^{-1} M H_2SO_4 and 10^{-3} M NaOH solutions.

A.c. impedance measurements were made on the rod specimen to determine the resistance and capacitance of the anodic oxide film as a function of film formation potential in the acidic and alkaline solutions. The measurements were performed with a Zahner IM5D impedance analyser by superimposing an a.c. signal of 5 mV amplitude on the d.c. potential over 1 to 10^5 Hz. The impedance data obtained were analysed by using the complex nonlinear least squares (CNLS) fitting method first described by Macdonald [16] and later modified in our laboratory [17].

A beam deflection technique was employed for the deflection measurements, which was developed by Stoney [18] and later modified by Nelson and Oriani [19]. The details of the beam deflection technique have been presented elsewhere [19, 20]. The deflection and the corresponding potential, which is just the film formation potential, were simultaneously measured with time during the anodic oxidation of the strip specimen at applied anodic current densities of 2 mA cm^{-2} and 10 mA cm^{-2} in the acidic and alkaline solutions. The applied current density was controlled by a constant current source (Hewlett-Packard 6181C), and the deflection and the film formation potential were recorded on a strip chart recorder (SOLTEC 1242). In addition, the film formation potential was obtained with time at various applied current densities (5–100 mA cm^{-2}) during the anodic oxidation of the rod specimen in the alkaline solution.

Results and discussion

Fig. 1a, b shows typical impedance spectra on the Nyquist plot obtained from the rod specimen at a film

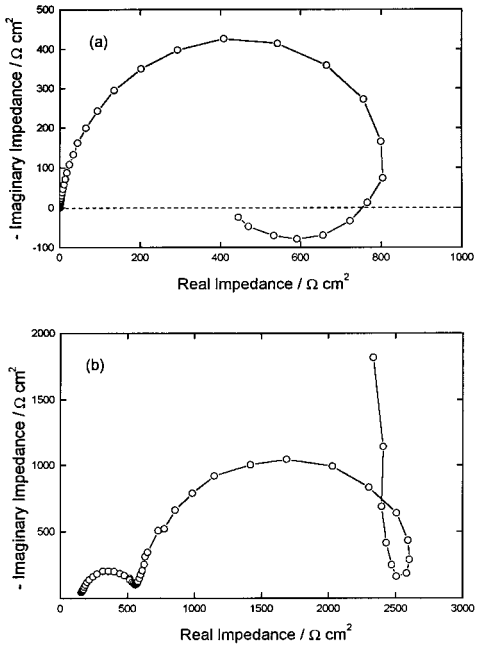

Fig. 1 a, b Typical Nyquist plots obtained from the pure aluminium rod specimen at an applied anodic potential of 0 V_{SCE} in **a** 5×10^{-1} M H_2SO_4 and **b** 10^{-3} M NaOH solutions

formation potential of 0 V_{SCE} in 5×10^{-1} M H_2SO_4 solution and 10^{-3} M NaOH solution, respectively. The impedance spectrum in the acidic solution consists of one capacitive semicircle in the high frequency region and one inductive semicircle in the low frequency region. The high-frequency capacitive semicircle represents the properties of the anodic oxide film and the low-frequency inductive semicircle is associated with an ionic relaxation phenomenon within the oxide film, which is due to time variations of O^{2-} ion build-up at the aluminium/oxide film interface [21]. By contrast, the impedance spectrum in the alkaline solution consists of two capacitive semicircles in high and intermediate frequency regions and one capacitive vertical line in the low frequency region. Fernandes et al. [22] suggested that the high and intermediate frequency capacitive semicircles represented a charge transfer process at the oxide/solution interface and the properties of anodic oxide film, respectively.

For the analyses of the measured impedance data in 5×10^{-1} M H_2SO_4 solution and 10^{-3} M NaOH solution, the electric equivalent circuits suggested by several authors [23, 24] and by Fernandes et al. [22], respectively, were employed. The CNLS data fitting [16, 17] was conducted on the basis of the equivalent circuits to determine the capacitance and resistance of anodic oxide films associated with the high-frequency semicircle in the acidic solution and with the intermediate-frequency semicircle in the alkaline solution.

The determined reciprocal capacitance and resistance of anodic oxide films in 5×10^{-1} M H_2SO_4 solution and 10^{-3} M NaOH solution are demonstrated as a function of film formation potential in Figs. 2 and 3, respectively.

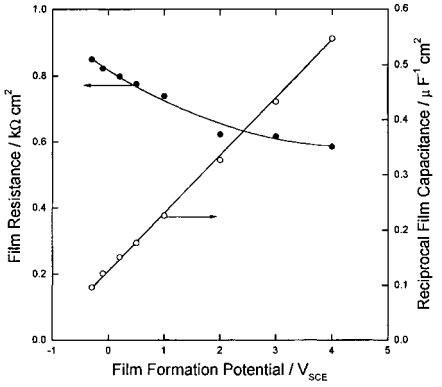

Fig. 2 Changes in the reciprocal capacitance (○) and resistance (●) of anodic oxide film on pure aluminium rod specimen with film formation potential in 5×10^{-1} M H_2SO_4 solution

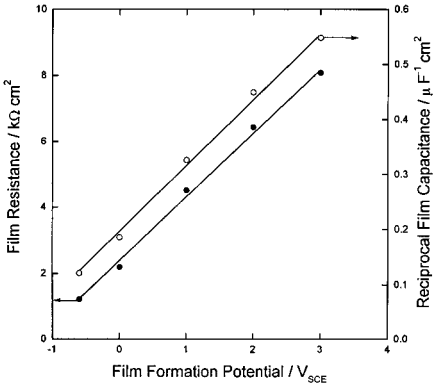

Fig. 3 Changes in the reciprocal capacitance (○) and resistance (●) of anodic oxide film on pure aluminium rod specimen with film formation potential in 10^{-3} M NaOH solution

The reciprocal film capacitance increased linearly with increasing film formation potential in both acidic and alkaline solutions. As the film formation potential increased, the film resistance decreased monotonically in the acidic solution, but it increased linearly in the alkaline solution.

The reciprocal film capacitance is generally accepted to be proportional only to the film thickness ℓ_{ox} according to [25]

$$\ell_{ox} = \varepsilon_o \varepsilon_{ox} A / C_{ox} \quad (1)$$

where ε_o is the vacuum permittivity (8.85×10^{-12} F m^{-1}), ε_{ox} is the relative permittivity of the oxide film, A is the exposed area of the specimen and C_{ox} represents the film capacitance. So, the increases in the reciprocal capacitance with film formation potential in both acidic and alkaline solutions (Figs. 2 and 3) are attributable to the increases in the film thickness with film formation potential. This is in good accordance with the fact that the film thickness on aluminium is linearly proportional to film formation potential [26].

The resistance of the anodic film on pure aluminium, R_{ox}, is related to ℓ_{ox} and the film resistivity ρ_{ox} according to Eq. 2:

$$R_{ox} = \rho_{ox} \ell_{ox} / A \quad (2)$$

The linear increase of the film resistance with film formation potential in alkaline solution (Fig. 3) is ascribed entirely to the growth of the oxide film, since the film thickness increased linearly with film formation potential. The film resistivity ρ_{ox} does not contribute to the change in the film resistance R_{ox} with film formation potential in alkaline solution.

However, the decrease in R_{ox} with film formation potential in acidic solution (Fig. 2) means that ρ_{ox} decreased significantly with increasing film formation potential. The preceding paper [24] reported that the decreased film resistivity arises from the increase in the vacancy concentration within the oxide film, which could be explained by a field-assisted dissolution of anodic oxide film at the oxide film/solution interface, which causes the generation of aluminium vacancies [14, 27]

$$Al_{Al}(ox) = Al^{3+}(aq) + V_{Al}^{3-}(ox) \quad (3)$$

where $Al_{Al}(ox)$ is the normal aluminium ion in the regular site of the oxide film, $Al^{3+}(aq)$ is the aluminium ion in aqueous solution and $V_{Al}^{3-}(ox)$ represents the negatively charged aluminium vacancy in the oxide film.

The transport number of cation in anodic oxide films on aluminium in neutral and slightly alkaline solutions was reported to be between 0.4 and 0.7, depending upon the applied current density [10, 11]. This implies the simultaneous presence of both cation and anion vacancies within the oxide film. In view of the fact that aluminium ions are not thermodynamically stable in alkaline solution [15], it is readily inferred that the generation of aluminium vacancy via the reaction of Eq. 3 hardly occurs in alkaline solution. Therefore, the generation of aluminium vacancy has been suggested by Pyun and Hong [8] to arise from another electrochemical reaction which is given by

$$H_2O(ad) = O_o(ox) + \tfrac{2}{3} V_{Al}^{3-}(ox) + 2H^+(aq) \quad (4)$$

where $H_2O(ad)$ is the adsorbed water on the oxide film surface, $O_o(ox)$ is the normal oxygen ion in the regular site of the oxide film and $H^+(aq)$ represents the hydrogen ion in the aqueous solution. The adsorption of water is scarcely influenced by the applied electric field, because water is an uncharged species, thus resulting in little change in the concentration of aluminium vacancy within the oxide film with film formation potential. This is why the film resistivity was not changed with film formation potential in alkaline solution (Fig. 3).

Chao et al. [6] suggested a point defect model in which the generation of cation vacancy was considered to result from the direct ejection of cations from the oxide film into the solution via the reaction of Eq. 3. In contrast, Pyun and Hong [8] showed that the adsorption of water via the reaction of Eq. 4 could contribute to the generation of cation vacancy. In this work, from the comparison of the dependence of the film resistance on

the film formation potential in acidic solution with that in alkaline solution, it is clearly shown that in acidic solution, cation vacancies are generated according to the model of Chao et al. [6], in which aluminium ions are directly ejected into the solution, but, in alkaline solution, they are produced through the adsorption of water on the oxide film surface according to Pyun and Hong's model [8], in which aluminate ions rather than aluminium ions are viable as a result of the dissolution of the oxide film.

Figure 4 presents the plots of the deflection and film formation potential of the strip specimen against time at an applied anodic current density of 2 mA cm^{-2} 5×10^{-1} M H_2SO_4 solution. The deflection moved monotonically towards a compressive direction. The film formation potential increased up to 50 s and then reached a steady-state value of about 9.5 V_{SCE}.

Figure 5 gives the deflection and film formation potential of the strip specimen as a function of time at an applied anodic current density of 2 mA cm^{-2} in 10^{-3} M NaOH solution. The deflection moved towards a compressive direction up to about 100s, after which it moved towards a tensile direction. The film formation potential increased up to 100 s and then reached a steady-state value of about 31 V_{SCE}.

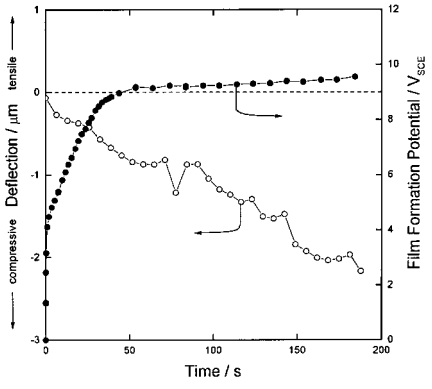

Fig. 4 Changes in the deflection (○) and film formation potential (●) obtained from the pure aluminium strip specimen with time at an applied anodic current density of 2 mA cm^{-2} in 5×10^{-1} M H_2SO_4 solution. The *dotted line* indicates the zero position of the deflection

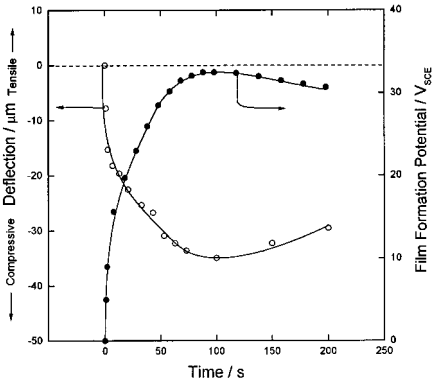

Fig. 5 Changes in the deflection (○) and film formation potential (●) obtained from the pure aluminium strip specimen with time at an applied anodic current density of 2 mA cm^{-2} in 10^{-3} M NaOH solution. The *dotted line* indicates the zero position of deflection

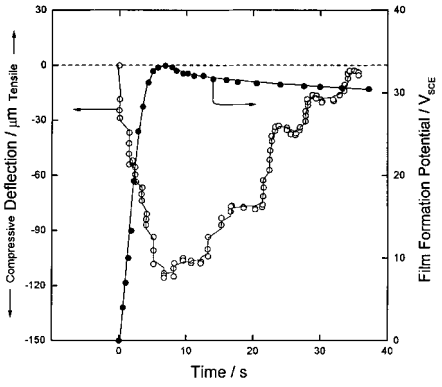

Fig. 6 Changes in the deflection (○) and film formation potential (●) obtained from the pure aluminium strip specimen with time at an applied anodic current density of 10 mA cm^{-2} in 10^{-3} M NaOH solution. The *dotted line* indicates the zero position of the deflection

Figure 6 depicts the time dependence of the deflection and film formation potential of the strip specimen at an applied anodic current density of 10 mA cm^{-2} in 10^{-3} M NaOH solution. The transition in the direction of movement of the deflection from compressive to tensile direction occurred at about 7 s. It is noted that the transition time, at which the deflection changes the direction in its movement from compressive to tensile, decreased with increasing applied anodic current density.

The mechanism for stress generation was suggested by Nelson and Oriani [20] to be related to the Philling-Bedworth Ratio (PBR) of the metal and the transport number of the ions in the oxide film. On the other hand, Kim et al. [28] introduced the point defect model of Chao et al. [6] to explain the stress generation mechanism. They attributed the generation of tensile stress during the growth of anodic oxide film on tungsten to the accumulation of oxygen vacancy at the metal/oxide film interface. In the preceding paper [23], we supplemented the concept of Kim et al. [28] to suggest a new model for stress generation during the growth of anodic oxide films, in which the developments of compressive and tensile stresses are attributed to the annihilation of cation vacancy and the generation of oxygen vacancy at the metal/oxide film interface, respectively.

Recognising that the generation rate of aluminium vacancy at the oxide film/solution interface in alkaline solution is much exceeded by that in acidic solution, as already mentioned in Figs. 2 and 3, it is plausible that an initial fast annihilation of aluminium vacancy occurs and is immediately followed by a rapid generation of oxygen vacancy at the aluminium/oxide film interface in alkaline solution. This will cause the deflection to be changed from a compressive to a tensile direction in its movement with time in alkaline solution, as shown in Figs. 5 and 6. However, since aluminium vacancies that are generated at the oxide film/solution interface are

supplied to the aluminium/oxide film interface in acidic solution, the annihilation rate of aluminium vacancy at the aluminium/oxide film interface would be low. This would cause the slow movement of the deflection in a compressive direction with time in acidic solution (Fig. 4).

Figure 7 illustrates the changes in film formation potential obtained from the rod specimen with time at various applied anodic current densities in 10^{-3} M NaOH solution. The film formation potential increased linearly with time up to a certain time and then reached a steady-state value of about 32 V_{SCE}, irrespective of the applied anodic current density. It was reported that gaseous oxygen is generated during anodising of aluminium above a film formation potential of 15 V [29]. In this work, gaseous oxygen was observed with the naked eye to evolve above a film formation potential of about 15 V_{SCE} in alkaline solution. Thus, the constant steady-state value of film formation potential independent of applied anodic current density in Fig. 7 is ascribed to oxygen evolution, for which the total charge transferred during the application of anodic current density is partly consumed. The rest of the charge will be used for the formation of anodic oxide film, and the rate of this process is counterbalanced by the chemical dissolution rate of the oxide film at the steady-state film formation potential, so that no growth of anodic oxide film occurs. This result does not give information about the distribution of both amounts of oxygen evolution and oxide film formation.

If the reaction of Eq. 4 is strongly retarded by the oxygen evolution in alkaline solution

$$2OH^- = \tfrac{1}{2}O_2 + H_2O + 2e \quad (5)$$

the time to transition of compressive to tensile deflection is much shortened. However, since the reaction of Eq. 5 is not coupled with the reaction of Eq. 4, one cannot say anything about what contribution of the oxygen evolution is made to the deflection developed during the growth of the anodic oxide film.

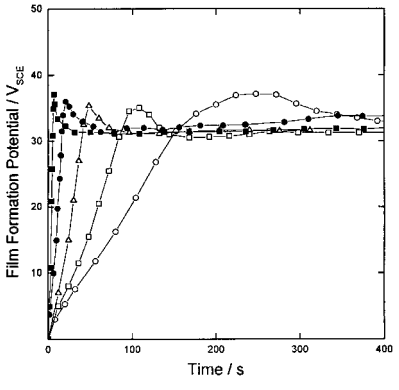

Fig. 7 Changes in film formation potential obtained from the pure aluminium rod specimen with time in 10^{-3} M NaOH solution at various applied anodic current densities of: ○, 5 mA cm^{-2}; □, 10 mA cm^{-2}; △, 20 mA cm^{-2}; ●, 50 mA cm^2; ■, 100 mA cm^{-2}

In summary, in this work the deflection data were qualitatively explained fairly well, based upon the model of the aluminium vacancy annihilation and oxygen vacancy generation at the metal/oxide film interface suggested in the preceding paper [24].

Conclusions

The growth mechanism of anodic oxide films on pure aluminium was investigated in aqueous acidic and alkaline solutions by using a.c. impedance spectroscopy and a beam deflection technique. The experimental results obtained in this work permit us to draw the following conclusions.

1. The reciprocal capacitance of an anodic oxide film on pure aluminium increased linearly with increasing film formation potential in both acidic and alkaline solutions, indicating the linear increase in the film thickness with film formation potential.
2. As the film formation potential increased, the resistance of the anodic oxide film decreased in acidic solution, while it increased in alkaline solution. This reveals that the generation of aluminium vacancy at the oxide film/solution interface is due to a field-assisted oxide dissolution in acidic solution, which involves direct ejection of aluminium ion from the oxide film into the solution, but is associated with the adsorption of water on the oxide film surface in alkaline solution, resulting in the formation of anodic oxide film.
3. The deflection was observed to move only towards a compressive direction with time in acidic solution. On the other hand, it showed a transition in the direction of movement from compressive to tensile stress in alkaline solution. The deflections generated during the growth of anodic oxide films were found to be closely related to the generation mechanism of aluminium vacancy at the oxide film/solution interface in acidic and alkaline solutions.
4. The film formation potential showed a steady-state value of about 32 V_{SCE} in 10^{-3} M NaOH solution, irrespective of applied current density. This implies that one portion of the total charge transferred during the application of anodic current density contributes to oxygen evolution, and the remainder accounts for the oxide formation around 32 V_{SCE}.

References

1. Cabrera N, Mott NF (1948) Rep Progr Phys 12: 267
2. Sato N, Cohen M (1964) J Electrochem Soc 111: 512
3. Vetter KJ, Gorn F (1973) Electrochim Acta 18: 321
4. Dignam MJ (1979) J Electrochem Soc 126: 2188
5. Young L, Smith DJ (1979) J Electrochem Soc 126: 765
6. Chao CY, Lin LF, Macdonald DD (1981) J. Electrochem Soc 128: 1187
7. Kirchheim R (1987) Electrochim Acta 32: 1619

8. Pyun S-I, Hong M-H (1992) Electrochim Acta 37: 327
9. Davies JA, Domeij B (1965) J Electrochem Soc 112: 675
10. Randall JJ Jr, Bernardo WJ (1975) 20: 653
11. Khalil N, Leach JSL (1986) Electrochim Acta 31: 1279
12. Diggle JW, Downie TC, Goulding CW (1969) J Electrochem Soc 116: 737
13. Patermarakis G, Lenas P, Karavassilis C, Papayiannis G (1991) Electrochim Acta 36: 709
14. Kim Y-S, Pyun S-I, Moon S-M, Kim J-D (1996) Corros Sci 38: 329
15. Pourbaix M (1974) Atlas of electrochemical equilibria in aqueous solutions. National Association of Corrosion Engineers, Houston, pp 168–176
16. Macdonald R (1972) Impedance spectroscopy. Wiley, New York
17. Bae J-S, Pyun S-I (1994) J Mater Sci Lett 13: 573
18. Stoney GG (1909) Proc Royal Soc A82: 172
19. Nelson JC, Oriani RA (1992) Electrochim Acta 37: 2051
20. Nelson JC, Oriani RA (1993) Corros Sci 34: 307
21. Lee S-M, Pyun S-I (1992) J Appl Electrochem 22: 151
22. Fernandes JCS, Ferreira MGS, Rangel CM (1990) J Appl Electrochem 20: 874
23. Lee E-J, Pyun S-I (1995) Corros Sci 37: 157
24. Moon S-M, Pyun S-I (1997) Electrochim Acta (submitted)
25. Diggle JW, Downie TC, Goulding CW (1969) Chem Rev 69: 365
26. Wernick S, Pinner R, Sheasby PG (1987) The surface treatment and finishing of aluminum and its alloys, vol 1. ASM International, Ohio, pp 290–313
27. Diggle JW, Downie TC, Goulding CW (1970) Electrochem Acta 15: 1079
28. Kim J-D, Pyun S-I, Oriani RA (1995) Electrochim Acta 40: 1171
29. Plumb RC (1958) J Electrochem Soc 105: 498